Correlation between the viscoelastic heterogeneity and the domain wall motion of Fe-based metallic glass

S. Ouyang,[1] L. J. Song,[1] Y. H. Liu,[2] J. T. Huo,[1,*] J. Q. Wang,[1,†] W. Xu,[1] J. L. Li,[3] C. T. Wang,[3] X. M. Wang,[1] and R. W. Li[1]

[1]*Key Laboratory of Magnetic Materials and Devices & Zhejiang Province Key Laboratory of Magnetic Materials and Application Technology, Ningbo Institute of Materials Technology & Engineering, Chinese Academy of Sciences, Ningbo, Zhejiang 315201, China*

[2]*Institute of Physics, Chinese Academy of Science, Beijing 100190, China*

[3]*Key Laboratory of Marine Materials and Related Technologies & Zhejiang Province Key Laboratory of Marine Materials and Protective Technologies, Ningbo Institute of Materials Technology & Engineering, Chinese Academy of Sciences, Ningbo, Zhejiang 315201, China*

(Received 12 December 2016; revised manuscript received 19 October 2017; published 1 June 2018)

The soft magnetic properties of Fe-based metallic glasses are reduced significantly by external and residual stresses, e.g., the susceptibility decreases and coercivity increases, which limits their application severely. Unraveling the micromechanism of how the stress influences the soft magnetic properties is of great help for enhancing the performance of Fe-based metallic glasses. In this work, we investigate the effect of viscoelastic heterogeneity on the motion of magnetic domain wall surrounding nanoindentations. Compared to the matrix, dissipation of the viscoelastic heterogeneity increases toward the nanoindentation. Meanwhile, the motion of domain wall under external magnetic field becomes more difficult toward the nanoindentations. A correlation between the viscoelastic dissipation and the moving ability of magnetic domain walls is observed, which can be well fitted using magnetoelastic coupling theory. This suggests that manipulating the microscale viscoelastic heterogeneity is probably a helpful strategy for enhancing the soft magnetic properties of metallic glasses.

DOI: 10.1103/PhysRevMaterials.2.063601

I. INTRODUCTION

Metallic glasses are a family of advanced materials that have been applied as soft magnetic materials, catalysts, and wear- and corrosion-resistant coatings [1–5]. The Fe-based metallic glasses with good soft magnetism have attracted considerable research interests and been widely applied in electrical industry. Extensive efforts have been done to explore new metallic glasses with excellent soft magnetic properties [6–8]. However, even for the same alloy composition, the soft magnetic properties of metallic glasses ribbon fabricated using different techniques can be distinct from each other. The residual stress, arising from nonequilibrium fabrication process and manufacture procedure, can reduce the soft magnetic performance of metallic glasses [9,10]. Appropriate annealing is generally able to release the residual stress and is helpful for improving soft magnetic properties [3,11,12]. But, annealing usually causes brittleness and it requires tremendous experimental work to obtain the optimal annealing procedure [13–15]. Unraveling the interaction mechanism between residual stress and magnetic properties can avoid these drawbacks caused by annealing and is helpful for optimizing the producing and manufacturing procedures of soft magnetic metallic glasses.

Even though it has obtained large success for studying the structure-properties relation for crystalline materials, it remains a challenge for metallic glasses due to the lack of suitable structure orders. A series of significant results have proved the existence of microstructural heterogeneity in metallic glasses [16–18]. The statistical analysis of the viscoelastic heterogeneity exhibits a good scaling character [16,19,20], which can be characterized quantitatively as an order parameter. Such viscoelastic heterogeneity is found to have close relation with other properties of metallic glasses, such as crystallization, flow units, and relaxation modes [20–22]. On the other hand, the macrosoft magnetic properties have been found to have close relation with the motion of magnetic domain walls [23,24]. It usually exhibits bad soft magnetic properties and requires larger external magnetic field to drive the movement of domain walls if there is coupling/pinning between the domain wall and structural heterogeneity (i.e., defects) [23,25,26]. Recent experimental results confirm that annealing is effective in modifying the viscoelastic heterogeneity [19,20]. This is probably associated with the change of soft magnetism upon annealing for Fe-based metallic glasses, which has yet to be verified. It is interesting to study whether the viscoelastic heterogeneity influences the motion of magnetic domain walls during magnetization.

In this work, the magnetic domains surrounding the nanoindentations of soft magnetic Fe-based metallic glasses are studied using magneto-optic Kerr microscope. The nanoscale viscoelastic heterogeneities surrounding the nanoindentations are studied using an amplitude-modulation atomic force microscope (AM-AFM). Clear correlation is found between the evolution of viscoelastic heterogeneity and the motion of domain wall under magnetic field. The underlying physical mechanism is analyzed quantitatively.

II. METHODS

The $Fe_{73.5}Si_{13.5}B_9Nb_3Cu_1$ ribbon was fabricated by the single-roller quenching method. The amorphous state was confirmed by the x-ray diffraction and differential scanning

*huojuntao@nimte.ac.cn
†jqwang@nimte.ac.cn

calorimetry. The free surface of as-spun ribbon with a mirror-like smoothness was studied in this work. The influence of surface roughness on phase shift is negligible; see Fig. S1 in Supplemental Material [27]. The magnetic domain structure was measured by digitally enhanced 950MT magneto-optic Kerr microscope in the mode of longitudinal Kerr effect with vertical sensitivity. The viscoelastic heterogeneity of the metallic glass ribbon was investigated using AM-AFM, produced by Bruker Company [16,19,20]. The probe tip is silicon with a force constant of about 40 N/m. The probe tip is very sharp with a curvature radius of about 2 nm, which is able to detect nanoscale heterogeneity. The energy dissipation ($E_{\rm dis}$) of viscoelasticity is calculated using the phase shift in AM-AFM measurement [28,29], $E_{\rm dis} = (\sin\varphi - \frac{A}{A_0}\frac{\omega}{\omega_0})\frac{\pi k A A_0}{Q}$, in which $E_{\rm dis}$ is the nanoscale energy dissipation; φ is the phase shift between the external excitation and the tip response; k is the spring constant of cantilever; Q is the quantity factor; A and A_0 represent the setpoint and free amplitude, respectively; ω and ω_0 represent the driving and resonant frequency. The energy dissipation of single-crystal silicon has a much narrower distribution that denotes a more homogeneous structure compared to Fe-based metallic glass; see Fig. S2 [27]. Indentations with different sizes from $r = 0.7$ to 1.8 μm were made on the free surface of ribbon using an MTS Nano Indenter G200 machine equipped with a Berkovich indenter; see Fig. S3 [27].

III. RESULTS

It is well known that an indent will cause stress gradient in its vicinity [30–32], especially when shear bands exist which can cause long-range stress gradient [33,34]. As shown in Figs. 1(a)–1(c), we make nanoindentations with different sizes on the surface of an $Fe_{73.5}Si_{13.5}B_9Nb_3Cu_1$ ribbon and control the nanoindentation dimension to manipulate the size of the stress gradient field. The energy density of a magnetic material can be expressed as $F = F_H + F_\sigma + F_w$ [35], where F_H is energy caused by external magnetic field, F_σ is magnetoelastic energy, F_w is domain wall energy. For equilibrium state of domain structure, $\delta F = \delta F_H + \delta F_\sigma + \delta F_w = 0$. When applying an indentation (at $\delta F_H = 0$), it causes stress gradient along the radial direction, with $\frac{\partial F_\sigma}{\partial r} \neq 0$ and $\frac{\partial F_\sigma}{\partial \zeta} \approx 0$ (r is the radial distance from indentation, ζ is the polar angle). The magnetoelastic energy is given as $F_\sigma = -\frac{3}{2}\lambda\sigma\cos\theta$, where λ is the magnetostriction constant, σ is stress, θ is the angle between stress and magnetization direction. To make the magnetoelastic energy minimum, the magnetization direction is always parallel or antiparallel to stress. Thus, it usually forms 180° domain wall which is confirmed by Kerr microscope. To keep the wall energy unchanged, $\delta F_w = -\delta F_\sigma = 0$, the domain wall tends to align with the contour of stress gradient in the ζ direction because of $\frac{\partial F_w}{\partial \zeta} = \frac{\partial F_\sigma}{\partial \zeta} \approx 0$. The radius ($R$) of the distorted magnetic domains surrounding the nanoindentation reflects the stress gradient radius. It can be seen that the size of the magnetic domain distortion increases with the indentation size (r). The R exhibits a linear relation with r, as shown in Fig. 1(d). For nanoindentations with radius from 0.7 to 1.8 μm, the R/r ratio remains about 7.9.

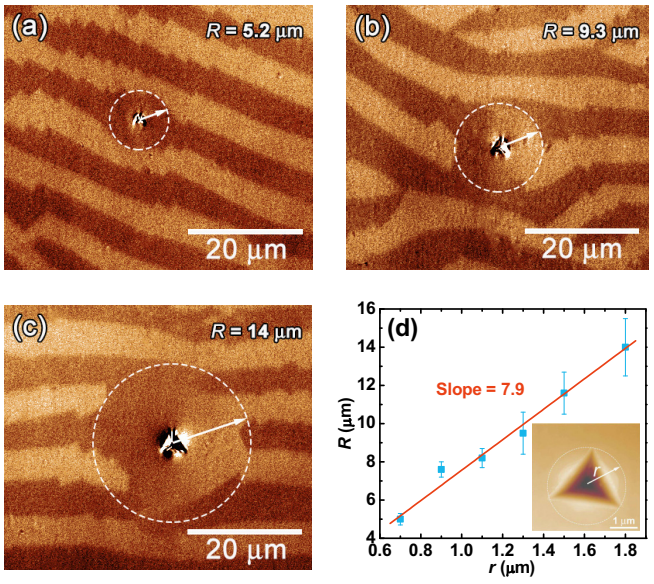

FIG. 1. The morphology of domain walls surrounding the nanoindentation. The indentation sizes are (a) $r = 0.7\,\mu$m, (b) $r = 1.1\,\mu$m, and (c) $r = 1.8\,\mu$m, respectively. The dashed circles highlight the radius (R) of the area with distorted domain walls. (d) The relation between R and r, which is well fitted by a linear equation with a slope of 7.9. Inset: a representative morphology of nanoindentation.

To study the influence of residual stress on domain wall, external magnetic fields are applied to measure the motion of domain wall around the indentations. As shown in Figs. 2(a)–2(h), the magnetization is determined by the moving of domain walls. For example, the domain wall moves by about $\Delta L = 1.7\ \mu$m when the magnetic field increases from 10 to 20 Oe. The moving ability of the domain wall under external magnetic field is defined by $\Delta L/\Delta H$, which is proportional to susceptibility [35–37]. Figure 2(i) shows $\Delta L/\Delta H$ versus the distance between domain wall and indentation. At zero external magnetic fields, the domain wall surrounding the indentation usually connects with the original stripelike domains; see Fig. 2(a). This induces large errors in determining the displacement of the domain wall. Thus, the data of $\Delta L/\Delta H$ when the external field increases from 0 to 10 Oe are not included in Fig. 2(i). It is found that the domain wall is more difficult to move when it gets closer to the nanoindentation, which denotes the decrease of susceptibility. We further found that when the external field is applied along the longitudinal direction (see Fig. S3 [27]), the value of $\Delta L/\Delta H$ is larger than that for the transversal direction, which confirms the shape anisotropic magnetization characters [9,38,39].

To detect the evolution of microstructure under the driving of nanoindentation, the viscoelastic behavior of the metallic glass is studied using AM-AFM. The $E_{\rm dis}$ represent the viscous character of metallic glass which is related to the concentration of flow units or free volume [40,41]. The viscoelastic behavior at different locations is measured along the line illustrated in Fig. 3(a). The corresponding energy dissipation images are displayed in Figs. 3(b)–3(f), respectively. The dimensions of each scanning image are about 175 × 175 nm. Close to the nanoindentation, the average $E_{\rm dis}$ is larger than that far from the nanoindentation. This suggests that the stressed metallic glasses close to nanoindentations become more viscous, which is consistent with Refs. [30,40].

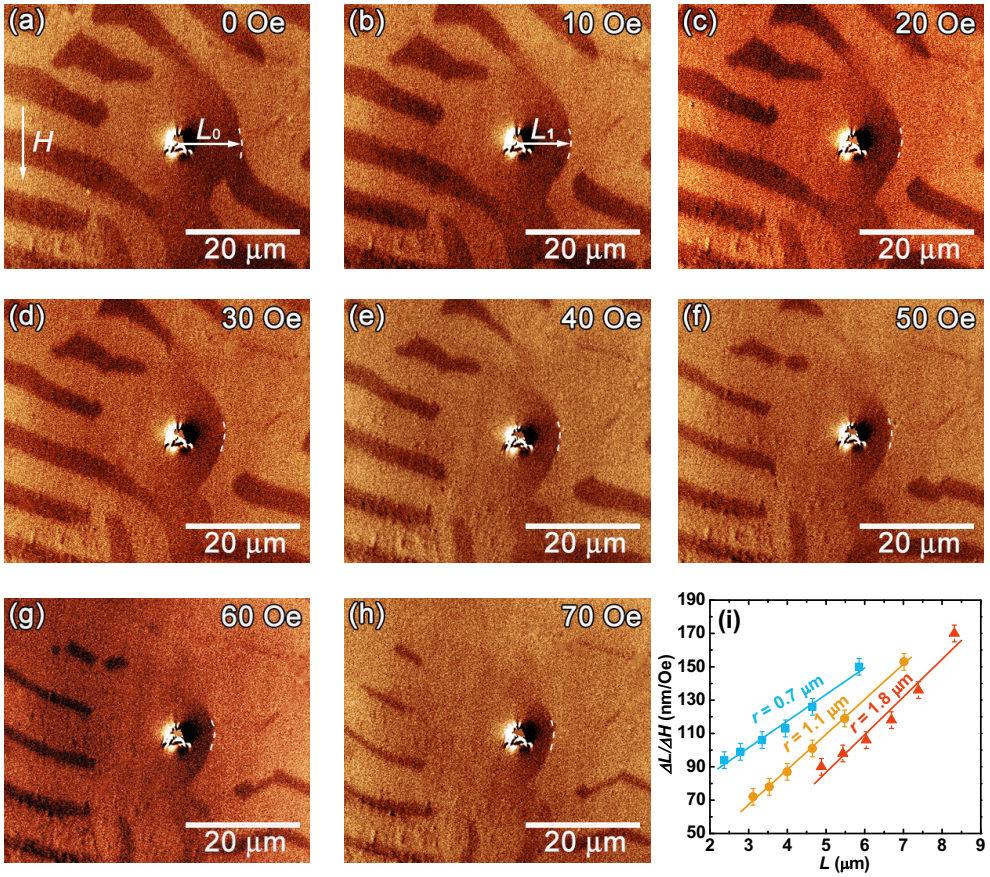

FIG. 2. Motion of domain walls under magnetic field. (a)–(h) The morphology of domain wall under the different magnetic fields, the nanoindentation is $r = 1.8\,\mu$m. The arrow on the left illustrates the magnetic field (H) direction. (i) The moving ability ($\Delta L/\Delta H$) of domain wall under transverse field for three nanoindentions with different dimensions.

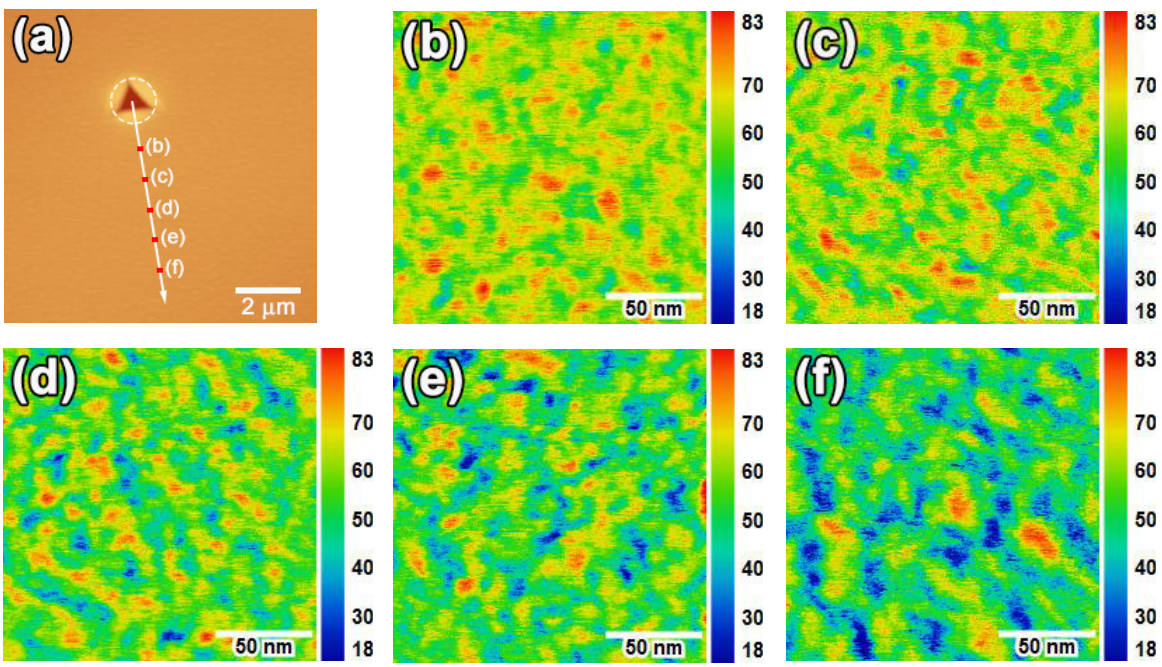

FIG. 3. Nanoscale viscoelastic heterogeneity surrounding the nanoindentation. (a) The illustration of positions for AFM measurements for the nanoindentation with $r = 0.7\,\mu$m. (b)–(f) The viscoelastic energy dissipation measured in different sites in parts (a), (b) $d = 1.7\,\mu$m, (c) $d = 2.7\,\mu$m, (d) $d = 3.7\,\mu$m, (e) $d = 4.7\,\mu$m, and (f) $d = 5.7\,\mu$m, respectively. The color bar represents the energy dissipation; unit is eV.

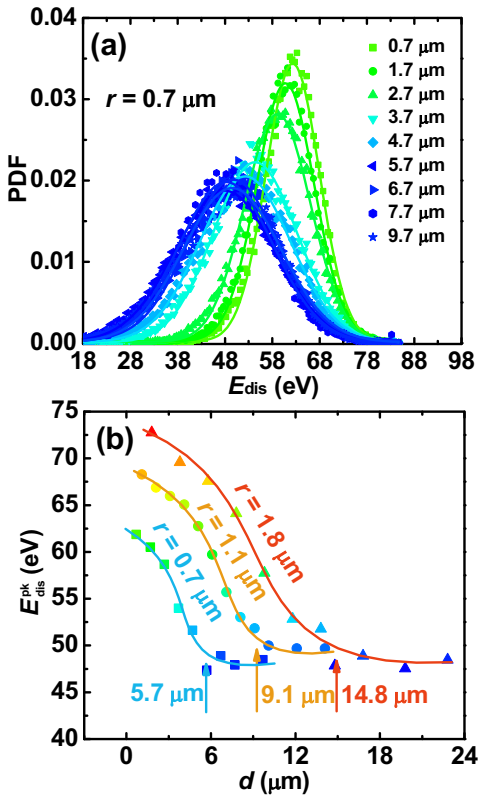

FIG. 4. (a) The probability density function (PDF) of energy dissipation and the Gaussian fitting for indentation with $r = 0.7\,\mu$m. (b) The peak value of the energy dissipation ($E_{\rm dis}^{\rm pk}$) versus the distance (d) from the nanoindentation center.

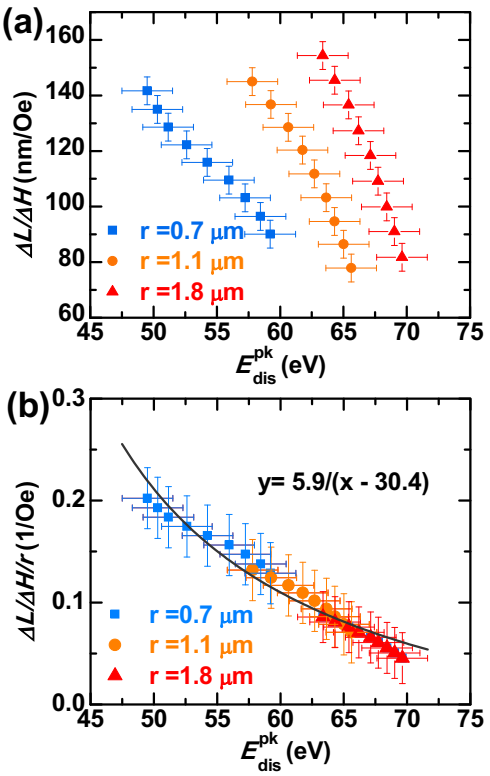

FIG. 5. Correlation between domain wall motion and dissipation energy. (a) The domain wall moving ability ($\Delta L/\Delta H$) versus the $E_{\rm dis}^{\rm pk}$. (b) The domain wall moving ability normalized by nanoindentation size ($\Delta L/\Delta H/r$) versus $E_{\rm dis}^{\rm pk}$, the data can be fitted by magnetoelastic coupling theory with equation of $y = 5.9/(x - 30.4)$.

Figure 4(a) presents the probability density function (PDF) of the dissipation energy surrounding nanoindentation with size of $r = 0.7\,\mu$m, which can be well fitted by Gaussian distribution. The dissipation energy PDF of other nanoindentations can be found in Fig. S5 [27]. Figure 4(b) shows the peak value of energy dissipation ($E_{\rm dis}^{\rm pk}$) versus the distance (d) from the nanoindentation center to the AFM measurement site. A larger nanoindentation induces larger dissipation energy. Away from the nanoindentation, the energy dissipation decreases and finally reaches a constant. The distance where the energy dissipation becomes a constant is determined to be about 5.7, 9.1, and 14.8 μm for nanoindentations with $r = 0.7, 1.1$, and 1.8 μm, respectively. These distances are in good consistence with the radii of domain distortion (R, shown in Fig. 1). This denotes that there may be correlation between the distortion of domain wall and the viscoelastic properties.

As shown in Fig. 5(a), the moving ability of domain wall ($\Delta L/\Delta H$) exhibits clear relation with the dissipation energy ($E_{\rm dis}^{\rm pk}$). This suggests that the viscoelastic behavior plays an important role in affecting the motion of magnetic domain walls. It is noteworthy that the data for three nanoindentations with different size in Fig. 5 do not overlap each other, which indicates that there are probably other factors also influencing the motion of magnetic domain walls. For example, structural defects (e.g., hole) without residual stress can also influence the motion of magnetic domains [42,43]. But, the radius of influence areas are about 3–4 times of the defect dimension [42], which are much smaller than the range observed here. It is interesting to find that if $\Delta L/\Delta H$ is normalized by the dimension (r) of the nanoindentation, the data overlap each other, as is shown in Fig. 5(b). Thus, the viscous character of metallic glasses probably plays an important role in controlling the motion of magnetic domain walls.

IV. MAGNETOELASTIC COUPLING THEORY ANALYSIS

For the magnetization controlled by the displacement of domain wall (confirmed in Fig. 2), it gives [35]

$$2\mu_0 M_s \Delta H = \frac{\partial^2 \gamma_w}{\partial x^2}\Delta L$$

and

$$\Delta M_H = 2M_s S_{\parallel} \Delta L.$$

The susceptibility is given as $\chi = \frac{\Delta M_H}{\Delta H} = \frac{4\mu_0 M_s^2}{\frac{\partial^2 \gamma_w}{\partial x^2}} S_{\parallel} = \frac{2M_s S_{\parallel}}{\Delta H}\Delta L$.

So, the mobility of domain wall under external field is proportional to the susceptibility (χ) $\Delta L/\Delta H/r = C_0\chi$, with $C_0 = \frac{1}{2M_s S_{\parallel}}$ a constant related to the saturated magnetization ($M_s = 1.24$ T [44]) and the area of domain wall ($S_{\parallel}$).

The susceptibility for stress-controlled domain wall motion is given by $\chi = \frac{C_1}{\sigma}$ [35], with $C_1 = \frac{2}{3\pi^2}\frac{la}{\delta\lambda_s}\mu_0 M_s^2$ a constant related to the saturated magnetization, $\lambda_s = 20 \times 10^{-6}$ is saturated magnetostriction constant [44], l is the width of

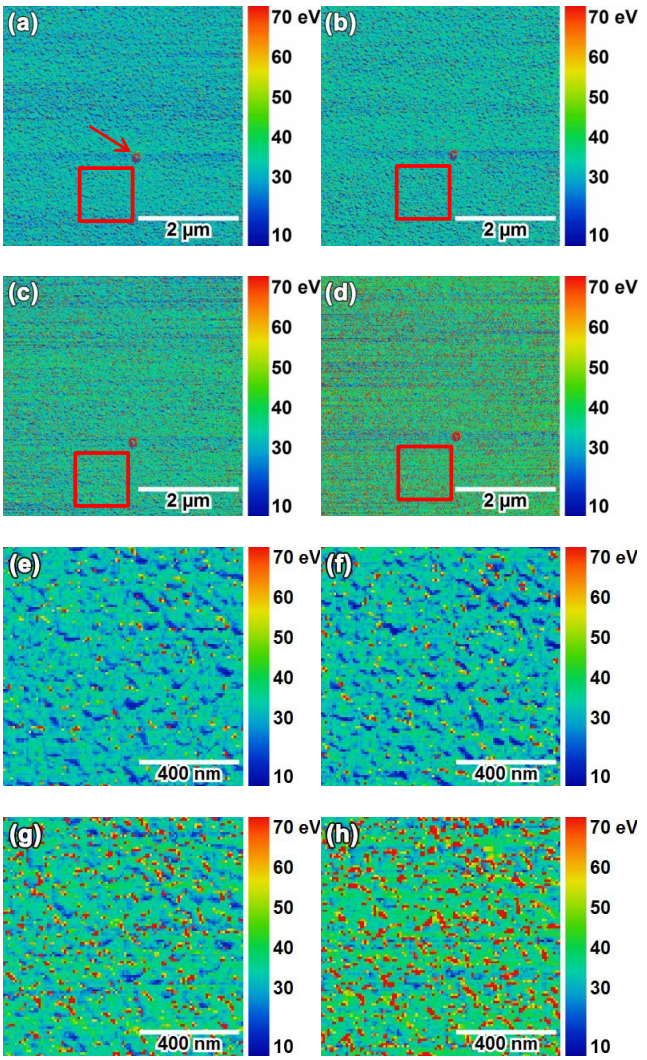

FIG. 6. (a)–(d) Low magnification AFM images at tensile states of $\gamma = 0, 0.33\%, 0.66\%$, and 1%, respectively. A mark (highlighted by the arrow) is selected to make sure the same area is studied. (e)–(h) High magnification AFM images for the same selected area [red squared zone in (a)–(d) images] at tensile states of $\gamma = 0, 0.33\%, 0.66\%$, and 1%, respectively.

magnetic domain, a represents the probability of a domain wall locating at stress minima and $S_{\parallel} = a/l$, δ is the thickness of domain wall.

To determine the stress quantitatively, we studied the viscoelastic characters *in situ* during tensile stress. A drawing clamp is designed to perform the tensile test, which is compatible with AFM test; see Fig. S6 [27]. The tensile displacement is controlled using a micrometer with a precision of 1 μm. The AFM images of viscoelastic characters at various tensile stresses are shown in Fig. 6. The statistical analysis about the dissipation energy is shown in Fig. 7. It is shown that the dissipation energy peak shifts to the larger $E_{\rm dis}$ side and the peak height decreases when the tensile stress increases. The relationship between the peak value of dissipation energy ($E_{\rm dis}^{\rm pk}$) and tensile strain is shown in Fig. 7(b), which can be well fitted using a linear equation $E_{\rm dis}^{\rm pk} = 300\gamma + 30.4$. Then, the relation between $E_{\rm dis}$ and stress is given as $E_{\rm dis} = C_2\sigma + C_3$, with $C_2 = 300/Y$ ($Y \approx 110$ GPa is the Young's modulus of metallic glass [45]), and $C_3 = 30.4$ are constants (see Fig. 7).

Then, it gives $\Delta L/\Delta H/r = \frac{C_0C_1C_2}{(E_{dis}-C_3)}$.

As shown in Fig. 5(b), this equation fits the experimental data well, with parameters of $C_0C_1C_2 = 5.9$ and $C_3 = 30.4$.

Furthermore, the thickness of domain wall (δ) can be estimated according to the fitting result of Fig. 5(b),

$$\begin{aligned} &5.9 \times 1.6 \times 10^{-19} \times 10^4 \\ &= C_0C_1C_2 = \frac{2}{3\pi^2}\frac{la}{\delta\lambda_s}\frac{\mu_0 M_s^2 300}{Y 2 M_s S_{\parallel}} \\ &= \frac{0.068l^2}{\delta \times 20 \times 10^{-6}}\frac{4\pi \times 10^{-7} \times 1.24^2 \times 300}{110 \times 10^9 \times 2 \times 1.24}. \end{aligned}$$

Given that the width of domain is about $l = 12\,\mu$m, see Figs. 1 and 2. The thickness (δ) of domain wall is estimated to be about

$$\begin{aligned} \delta &= \frac{1}{5.9 \times 1.6 \times 10^{-19} \times 10^4} \\ &\times \frac{0.068 \times \left(12 \times 10^{-6}\right)^2 \times 4\pi \times 10^{-7} \times 1.24^2 \times 300}{20 \times 10^{-6} \times 110 \times 10^9 \times 2 \times 1.24} \\ &= 36 \times 10^{-9}\,\text{m}. \end{aligned}$$

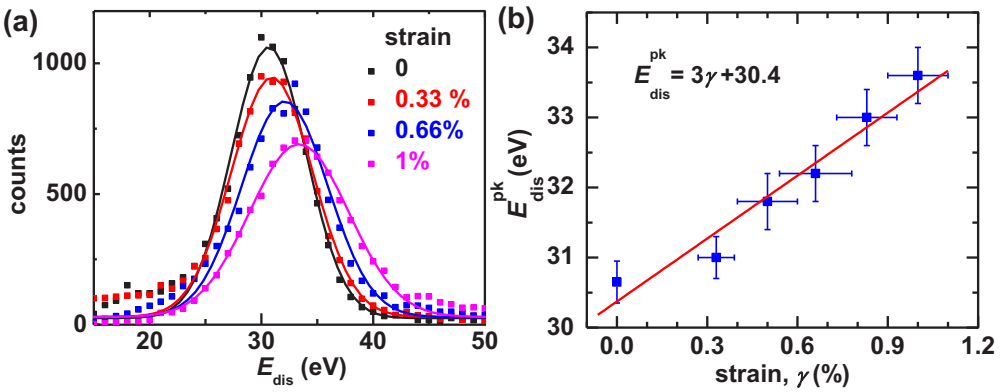

FIG. 7. (a) Statistical counts versus dissipation energy ($E_{\rm dis}$) for representative tensile states (tensile strain: 0, 0.33%, 0.66%, and 1%). The solid curves are fitting results by Gaussian equation. (b) The peak value of dissipation energy ($E_{\rm dis}^{\rm pk}$) versus tensile strain (γ). The data can be fitted well by linear equation $E_{\rm dis}^{\rm pk} = 3\gamma + 30.4$.

It is noteworthy that the thickness of the domain wall is comparable to the size of zones with high dissipation energy (flow units), which suggests that there are probable coupling effects between them. It has been believed that the domain walls in soft magnetic metallic glasses are wide, and nanoscale inhomogeneity can be averaged out [3]. However, our results confirm that the thickness of the domain wall is comparable to the characteristic dimension of viscoelastic heterogeneity which cannot be averaged out.

In summary, we have studied the influence of the residual stress surrounding the nanoindentation on the motion of magnetic domain wall of an Fe-based metallic glass. We find that the viscoelastic heterogeneity is a good parameter to characterize the change of structure under stress. A correlation between the viscoelastic heterogeneity and motion of domain walls is observed, which can be well fitted by the magnetoelastic coupling theory. The viscoelastic heterogeneity is a key character influencing the mobility of the domain wall and an important parameter for evaluating the strength of magnetoelastic effect in metallic glasses. These results suggest that manipulation of the nanoscale viscoelasticity is probably a new route to improve the soft magnetic properties of metallic glasses.

ACKNOWLEDGMENTS

The financial support from National Natural Science Foundation of China (NSFC Grants No. 51771216, No. 11504391, No. 51771217, and No. 51701230), Zhejiang Provincial Natural Science Foundation of China (Grants No. LR18E010002 and No. LY17E010005), National Key R&D Program of China (Grant No. 2016YFA0201102), and One Hundred Talents Program of Chinese Academy of Sciences are acknowledged. J.Q.W. and J.T.H. conceived this work. S.O. did the experiments. L.J.S. and Y.H.L. helped in preparing the figures. J.L.L. and C.T.W. assisted in doing the nanoindentation experiments. All authors discussed the results and contributed in writing the paper.

[1] Y. C. Hu, Y. Z. Wang, R. Su, C. R. Cao, F. Li, C. W. Sun, Y. Yang, P. F. Guan, D. W. Ding, Z. L. Wang, and W. H. Wang, Adv. Mater. **28**, 10293 (2016).
[2] J. Q. Wang, Y. H. Liu, M. W. Chen, G. Q. Xie, D. V. Louzguine-Luzgin, A. Inoue, and J. H. Perepezko, Adv. Funct. Mater. **22**, 2567 (2012).
[3] T. Egami, Rep. Prog. Phys. **47**, 1601 (1984).
[4] A. Inoue and A. Takeuchi, Acta Mater. **59**, 2243 (2011).
[5] S. Tanaka, T. Kaneko, N. Asao, Y. Yamamoto, M. Chen, W. Zhang, and A. Inoue, Chem. Commun. **47**, 5985 (2011).
[6] A. Makino, T. Kubota, M. Makabe, C. T. Chang, and A. Inoue, Mater. Sci. Eng. B **148**, 166 (2008).
[7] A. D. Wang, C. L. Zhao, A. N. He, H. Men, C. T. Chang, and X. M. Wang, J. Alloys Compd. **656**, 729 (2016).
[8] A. Inoue, B. L. Shen, H. Koshiba, H. Kato, and A. R. Yavari, Nat. Mater. **2**, 661 (2003).
[9] Z. H. Tang, B. M. Wang, H. L. Yang, X. Y. Xu, Y. W. Liu, D. D. Sun, L. X. Xia, Q. F. Zhan, B. Chen, M. H. Tang, Y. C. Zhou, J. L. Wang, and R. W. Li, Appl. Phys. Lett. **105**, 103504 (2014).
[10] M. L. Spano, J. Appl. Phys. **53**, 2667 (1982).
[11] M. Carara, M. N. Baibich, and R. L. Sommer, J. Appl. Phys. **91**, 8441 (2002).
[12] T. Jagielingski, IEEE Trans. Magn. **19**, 1925 (1983).
[13] J. Q. Wang, Y. Shen, J. H. Perepezko, and M. D. Ediger, Acta Mater. **104**, 25 (2016).
[14] G. Kumar, P. Neibecker, Y. H. Liu, and J. Schroers, Nat. Commun. **4**, 1536 (2013).
[15] M. Aljerf, K. Georgarakis, and A. R. Yavari, Acta Mater. **59**, 3817 (2011).
[16] Y. H. Liu, D. Wang, K. Nakajima, W. Zhang, A. Hirata, T. Nishi, A. Inoue, and M. W. Chen, Phys. Rev. Lett. **106**, 125504 (2011).
[17] H. Wagner, D. Bedorf, S. Küchemann, M. Schwabe, B. Zhang, W. Arnold, and K. Samwer, Nat. Mater. **10**, 439 (2011).
[18] W. Dmowski, T. Iwashita, C. P. Chuang, J. Almer, and T. Egami, Phys. Rev. Lett. **105**, 205502 (2010).
[19] Y. Yang, J. F. Zeng, A. Volland, J. J. Blandin, S. Gravier, and C. T. Liu, Acta Mater. **60**, 5260 (2012).
[20] F. Zhu, H. K. Nguyen, S. X. Song, D. P. B. Aji, A. Hirata, H. Wang, K. Nakajima, and M. W. Chen, Nat. Commun. **7**, 11516 (2016).
[21] W. Schirmacher, G. Ruocco, and V. Mazzone, Phys. Rev. Lett. **115**, 015901 (2015).
[22] T. Ichitsubo, E. Matsubara, T. Yamamoto, H. S. Chen, N. Nishiyama, J. Saida, and K. Anazawa, Phys. Rev. Lett. **95**, 245501 (2005).
[23] A. Pérez-Junquera, V. I. Marconi, A. B. Kolton, L. M. Alvarez-Prado, Y. Souche, A. Alija, M. Velez, J. V. Anguita, J. M. Alameda, J. I. Martin, and J. M. R. Parrondo, Phys. Rev. Lett. **100**, 037203 (2008).
[24] R. H. Yu, S. Basu, Y. Zhang, and J. Q. Xiao, J. Appl. Phys. **85**, 6034 (1999).
[25] U. Welp, V. K. Vlasko-Vlasov, G. W. Crabtree, C. Thompson, V. Metlushko, and B. Ilic, Appl. Phys. Lett. **79**, 1315 (2001).
[26] A. Budruk, C. Phatak, A. K. Petford-Long, and M. De Graef, Acta Mater. **59**, 6646 (2011).
[27] See Supplemental Material at http://link.aps.org/supplemental/10.1103/PhysRevMaterials.2.063601 for the comparison between surface roughness and phase shift, phase shift comparison for metallic glass and single crystalline Si, load-displacement curves for nanoindentations, further domain wall motion, further viscoelastic heterogeneity, and image of the *in situ* drawing clamp.
[28] R. Garcia, C. J. Gómez, N. F. Martinez, S. Patil, C. Dietz, and R. Magerle, Phys. Rev. Lett. **97**, 016103 (2006).
[29] R. Garcia, R. Magerle, and R. Perez, Nat. Mater. **6**, 405 (2007).
[30] C. A. Schuh, T. C. Hufnagel, and U. Ramamurty, Acta Mater. **55**, 4067 (2007).
[31] R. Vaidyanathan, M. Dao, G. Ravichandran, and S. Suresh, Acta Mater. **49**, 3781 (2001).
[32] J. Q. Wang and J. H. Perepezko, J. Chem. Phys. **145**, 211803 (2016).
[33] R. Maaß, K. Samwer, W. Arnold, and C. A. Volkert, Appl. Phys. Lett. **105**, 171902 (2014).

[34] R. Maaß, P. Birckigt, C. Borchers, K. Samwer, and C. A. Volkert, Acta Mater. **98**, 94 (2015).
[35] D. F. Wan and X. L. Ma, *Magnetic Physics* (University of Electronic Science and Technology of China Press Chengdu, China, 1994), pp. 300–305.
[36] E. Lopatina, I. Soldatov, V. Budinsky, M. Marsilius, L. Schultz, G. Herzer, and R. Schafer, Acta Mater. **96**, 10 (2015).
[37] R. S. Turtelli, J. P. Sinnecker, R. Grössinger, G. Badurek, C. Kussbach, and P. Allia, Phys. Rev. B **63**, 094427 (2001).
[38] G. Herzer, IEEE Trans. Magn. **30**, 4800 (1994).
[39] G. H. Dai, Q. F. Zhan, H. L. Yang, Y. W. Liu, X. S. Zhang, Z. H. Zuo, B. Chen, and R. W. Li, J. Appl. Phys. **114**, 173913 (2013).
[40] J. C. Ye, J. Lu, C. T. Liu, Q. Wang, and Y. Yang, Nat. Mater. **9**, 619 (2010).
[41] W. H. Wang, Y. Yang, T. G. Nieh, and C. T. Liu, Intermetallics **67**, 81 (2015).
[42] Y. Inada, Z. Akase, D. Shindo, and A. Taniyama, Mater. Trans. **53**, 1330 (2012).
[43] A. Pérez-Junquera, J. I. Martín, M. Vélez, J. M. Alameda, J. V. Anguita, F. Briones, E. M. González, and J. L. Vicent, Nanotechnology **15**, S131 (2004).
[44] Y. Yoshizawa, S. Oguma, and K. Yamauchi, J. Appl. Phys. **64**, 6044 (1988).
[45] M. Song, Y. Y. Sun, and Y. H. He, Mater. Sci. Eng. A **556**, 974 (2012).